Report

Cell Reports

Intercellular Calcium Signaling Induced by ATP Potentiates Macrophage Phagocytosis

Graphical Abstract

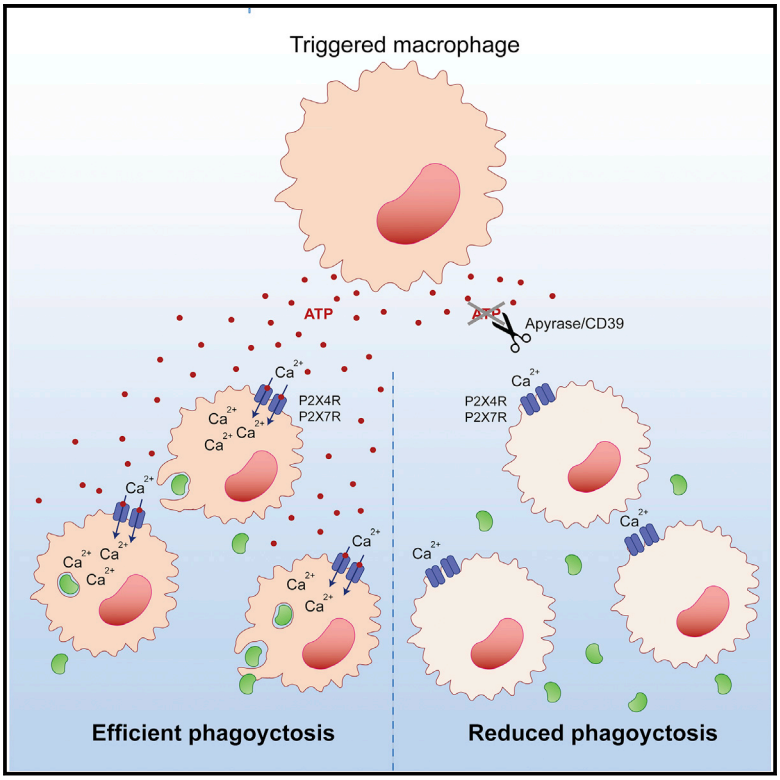

Authors

Sara Zumerle, Bianca Calì, Fabio Munari, Roberta Angioni, Francesco Di Virgilio, Barbara Molon, Antonella Viola

Correspondence

sara.zumerle@unipd.it

In Brief

Exchange of information is critical for an efficient immune response. Here, Zumerle et al. show that macrophages exploit ATP release as a paracrine communication mechanism to propagate calcium signals to neighboring cells. Signal propagation relies on P2X4 and P2X7 receptors and sustains macrophage phagocytosis.

Highlights

- Triggered macrophages release ATP-inducing Ca^{2+} spikes in resting bystander cells
- Calcium signal propagation is mediated by P2X4 and P2X7 receptors
- ATP-dependent paracrine communication is a feature of pro-inflammatory macrophages
- Paracrine ATP signaling is required for efficient phagocytosis

Zumerle et al., 2019, Cell Reports *27*, 1–10
April 2, 2019
https://doi.org/10.1016/j.celrep.2019.03.011

CellPress

Cell Reports
Report

Intercellular Calcium Signaling Induced by ATP Potentiates Macrophage Phagocytosis

Sara Zumerle,[1,2,5,*] Bianca Calì,[1,2] Fabio Munari,[1,2] Roberta Angioni,[1,2] Francesco Di Virgilio,[3] Barbara Molon,[1,4] and Antonella Viola[1,2]
[1]Department of Biomedical Sciences, University of Padova, Padova, Italy
[2]Fondazione Istituto di Ricerca Pediatrica Città della Speranza, Padova, Italy
[3]Department of Morphology, Surgery and Experimental Medicine, University of Ferrara, Ferrara, Italy
[4]Veneto Institute of Molecular Medicine, Padova, Italy
[5]Lead Contact
*Correspondence: sara.zumerle@unipd.it
https://doi.org/10.1016/j.celrep.2019.03.011

SUMMARY

Extracellular ATP is a signaling molecule exploited by the immune cells for both autocrine regulation and paracrine communication. By performing live calcium imaging experiments, we show that triggered mouse macrophages are able to propagate calcium signals to resting bystander cells by releasing ATP. ATP-based intercellular communication is mediated by P2X4 and P2X7 receptors and is a feature of pro-inflammatory macrophages. In terms of functional significance, ATP signaling is required for efficient phagocytosis of pathogen-derived molecules and apoptotic cells and may represent a target for macrophage regulation by CD39-expressing cells. These results highlight a cell-to-cell communication mechanism tuning innate immunity.

INTRODUCTION

Macrophages play a pivotal role in defending our organism from infectious agents and participate in development, tissue remodelling, and in the establishment and maintenance of inflammation. Among macrophage effector functions, phagocytosis is the most characterizing one, being the feature that led to their identification (Underhill et al., 2016). Importantly, macrophages are able to phagocytose a wide array of target particles: foreign particles, such as pathogens that need to be eliminated, but also apoptotic cells and cellular debris, a key process for the maintenance of tissue homeostasis (Lim et al., 2017).

Following the activation triggered by phagocytosis, macrophages produce several inflammatory mediators, such as cytokines, chemokines, and other signaling molecules, ensuring an efficient intercellular communication. This phenomenon is pivotal for the organization and coordination of different immune cells (Rivera et al., 2016). On the other hand, macrophages are characterized by remarkable plasticity, tuning their response according to the extracellular cues they receive. For these reasons, they are outstanding regulators of the immune response.

Among the signaling molecules released within the inflammatory microenvironment, ATP functions as an autocrine and paracrine modulator of several cell responses, thanks to the interaction with dedicated receptors, the purinergic P2 receptors (Khakh and Burnstock, 2009). Purinergic signaling plays an important role during inflammation. Damaged and necrotic tissues discharge large quantities of ATP, and immune cells can release it in a controlled fashion (Idzko et al., 2014; Junger, 2011). Macrophages, in particular, have been shown to release ATP in response to microbial stimuli (Cohen et al., 2013; Ren et al., 2014; Xiang et al., 2013), uric acid, and silica and alum crystals (Riteau et al., 2012), as well as following osmotic and mechanical stress (Burnstock and Knight, 2017; Burow et al., 2015). Several mechanisms have been proposed for ATP release: vesicular transport and exocytosis (Ren et al., 2014; Sakaki et al., 2013), connexin and pannexin hemichannels (Beyer and Steinberg, 1991; Riteau et al., 2012; Yang et al., 2015), anion channels (Burow et al., 2015), or P2X7 itself (Pellegatti et al., 2005). Thus, the inflammatory microenvironment is typically ATP rich, and, in this context, the nucleotide is considered an alarm-signaling molecule (Idzko et al., 2014).

We have recently shown that ATP can be exploited as a paracrine signaling molecule by T lymphocytes, allowing cell-to-cell communication via the propagation of calcium waves within lymph nodes (Wang et al., 2014). ATP-induced propagation of calcium signals has also been described in other cell types and tissues and provides an outstanding mechanism for the rapid spreading of information (Cotrina et al., 1998; Guthrie et al., 1999; Osipchuk and Cahalan, 1992; Zsembery et al., 2003).

Despite the effects of extracellular ATP on macrophages, which have been described in many studies, it is currently unknown whether macrophages exploit ATP release as an intercellular communication mechanism. In addition, the role of extracellular ATP on macrophage phagocytic activity is unknown. Thus, the aim of this work is to investigate ATP-mediated paracrine signaling among macrophages within lymphoid tissue and to assess its impact on macrophage functions.

RESULTS

Macrophages Propagate Calcium Signals by Releasing Extracellular ATP

The increase of intracellular calcium has been observed downstream of several signaling pathways in macrophages, such as FcγR, innate immunoreceptors, and chemokine receptors (Feske et al., 2015). Using cell-membrane-permeable caged

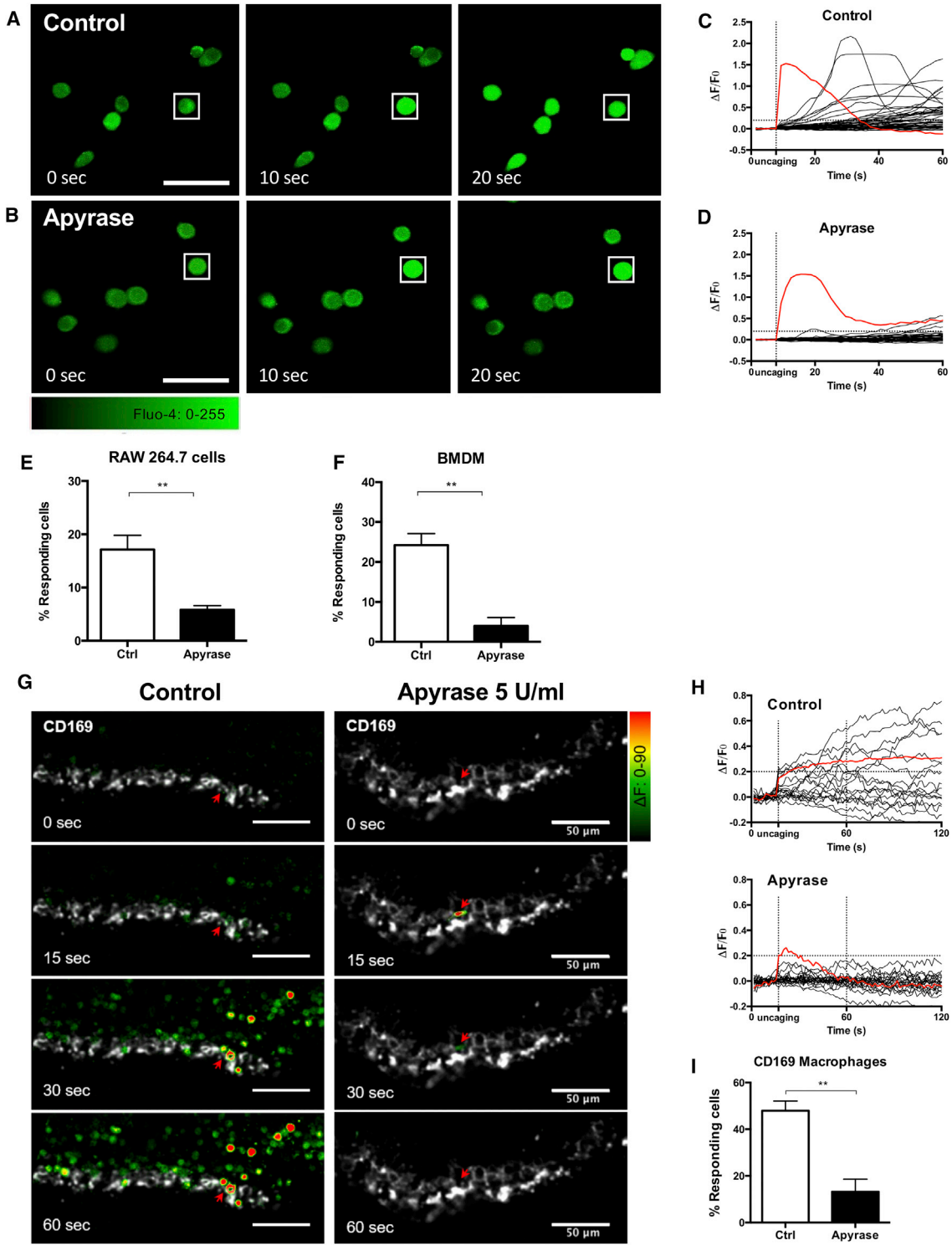

Figure 1. Macrophages Propagate Calcium Signals in an ATP-Dependent Manner

(A and B) Murine RAW 264.7 macrophages were loaded with photoactivatable caged-IP_3 and the fluorescent calcium indicator Fluo-4 (green). An intracellular calcium wave was initiated by laser-mediated photolysis on a single cell (white box indicates uncaging), and its propagation to bystander cells was monitored in terms of cytosolic calcium increase (green fluorescence). Experiments were performed in Hank's balanced salt solution (HBSS) with 2 mM Ca^{2+} in the absence (A) or presence (B) of the ATP-hydrolyzing enzyme apyrase (5 U/mL). Scale bars, 50 μm. See also Video S1.

(legend continued on next page)

IP_3 (Li et al., 1998), we triggered an intracellular single-cell Ca^{2+} increase in bone-marrow-derived macrophages (BMDMs) and in the murine cell line RAW 264.7 using a short UV laser pulse (uncaging) (Figure 1). Interestingly, we clearly observed calcium signal propagation to bystander cells that were not in contact with the triggered one (Figures 1A–1C; Videos S1 and S2), suggesting that calcium waves were propagated through a soluble mediator. The UV pulse itself did not trigger the calcium signal propagation, as it was not observed in cells loaded with the calcium indicator but lacking caged-IP_3 (data not shown).

We recently discovered that T lymphocytes exploit ATP as a paracrine signaling molecule (Wang et al., 2014). Several studies show that macrophages release ATP in response to microbial stimuli (Cohen et al., 2013; Ren et al., 2014), and we hypothesized that ATP may be involved in macrophage paracrine signaling regulation. Thus, we repeated the experiments described earlier in the presence of the ATP-hydrolyzing enzyme apyrase (Figures 1B–1D; Videos S1 and S2). In these conditions, we could not detect calcium paracrine signaling among macrophages, as indicated by the very low number of bystander cells responding after the triggered one (Figures 1E and 1F); importantly, apyrase treatment did not affect the calcium spike of the irradiated cell (Figures S1A and S1B). Altogether, these results indicate that, in response to intracellular calcium increase, macrophages release ATP that induces calcium signaling in unstimulated, neighboring cells.

To assess the existence of this ATP-based calcium signal propagation in a more physiological context, we performed calcium imaging experiments *ex vivo*, in viable lymph node slices (Wang et al., 2014). We focused on subcapsular macrophages, visualized by the use of a fluorescently conjugated anti-CD169 antibody that was subcutaneously injected 1 h before collecting the popliteal lymph nodes used for the experiments (Carrasco and Batista, 2007; Junt et al., 2007). The staining of CD169-positive cells was specific, as demonstrated by the expected subcapsular localization and by the absence of fluorescent signal in control experiments performed using a fluorescently labeled isotype (Figure S1C).

The propagation of calcium signals was observed also in this experimental setting and was abolished by the addition of apyrase (Figure 1G; Video S3). The UV pulse did not induce the propagation of calcium signals, as demonstrated by appropriate control experiments (Figure S1D).

Altogether, these data indicate that signals inducing IP_3-mediated calcium release from intracellular stores in macrophages result in the release of ATP, which then stimulates calcium signaling in the neighboring cells, acting as a paracrine signaling amplifier.

P2X4 and P2X7 Purinergic Receptors Are Involved in ATP-Dependent Paracrine Signaling

Extracellular ATP is the principal ligand of the large family of purinergic receptors, which are expressed by several populations of cells. Purinergic receptors are classified in two distinct subfamilies, named P2X and P2Y. Upon ligand binding, both receptor subfamilies induce an increase of cytosolic calcium but through two distinct mechanisms: the P2X receptors form cation-permeable channels in the plasma membrane leading to the influx of extracellular calcium, while the P2Y proteins activate a signaling cascade resulting in calcium release from the intracellular stores (Idzko et al., 2014). Thus, to determine which purinergic receptor subfamily is involved in the ATP-based paracrine signaling between macrophages, we performed the live calcium imaging experiments in a calcium-free extracellular solution, supplemented with the calcium chelator EGTA. Importantly, although the absence of extracellular calcium reduced the overall Fluo-4-AM fluorescent signal, the IP_3 uncaging induced a calcium spike in the pulsed cell comparable to that in the control condition (Figures 2A and 2B). However, the percentage of bystander cells responding to the triggered one was markedly reduced in the Ca^{2+}-free environment, indicating that extracellular calcium is required for the signal propagation (Figures 2C and 2D; Video S4). This result suggests that purinergic receptors belonging to the P2X subfamily are involved in ATP-based paracrine signaling.

It has been reported that macrophages mainly express P2X4 and P2X7 receptors (P2X4R and P2X7R) but can also express functional P2X1R and P2X2R (Burnstock, 2016; Coutinho-Silva et al., 2005; Sim et al., 2007). In BMDMs and in RAW 264.7 cells, the cells used for the calcium imaging experiments, P2X1R and P2X2R mRNAs were not detectable, whereas both P2X4R and P2X7R mRNAs were expressed (Figures 2E and 2F). We also analyzed their presence in lymph nodes and confirmed the expression of both the receptors by subcapsular macrophages (Figure S2).

To assess their role in ATP-based paracrine communication, we performed live calcium imaging experiments in the presence of selective chemical antagonists for these receptors and found that the blockage of either P2X4 or P2X7 receptors reduced the calcium signal propagation (Figure 2G). To corroborate these results, we genetically modulated the receptors' expression by using specific small interfering RNA (siRNA). Despite extensive

(C and D) Quantification of live calcium imaging experiments performed in the absence (C) or presence (D) of apyrase was realized by counting the percentage of bystander cells (black traces) whose variation of fluorescence was above the threshold ($\Delta F/F_0 > 0.2$) after the uncaging of the origin cell (red trace).

(E and F) Quantification of 3 independent live calcium imaging experiments conducted with murine cell line RAW 264.7 (E) and primary bone-marrow-derived macrophages (F). Error bars represent SEM. For data analysis, Student's t test was used (**$p < 0.01$). See also Videos S1 and S2.

(G) Fresh murine popliteal lymph nodes were enclosed in 4% agarose gel, cut into 200-μm slices, and loaded with caged-IP_3 and Fluo-4-AM (shown in false colors), before performing live calcium imaging experiments as described in (A). Subcapsular macrophages were visualized by a fluorescently labeled anti-CD169 antibody (gray), subcutaneously injected 1 h before the experiment. The arrows indicate the cells irradiated with the UV laser (uncaging). The Fluo-4 baseline fluorescence of the first frames (before the uncaging) was subtracted from all the frames. The fluorescence variation is shown in false colors (ΔF 0–90). Scale bar, 50 μm. See also Video S3.

(H) Representative traces of live calcium imaging experiments, showing the fluorescence variation after the uncaging of the origin cell (red) and the bystander macrophages (black).

(I) Quantification of 5 independent live calcium imaging experiments, performed with lymph nodes from 5 animals. Error bars represent SEM. For data analysis, Student's t test was used (**$p < 0.01$).

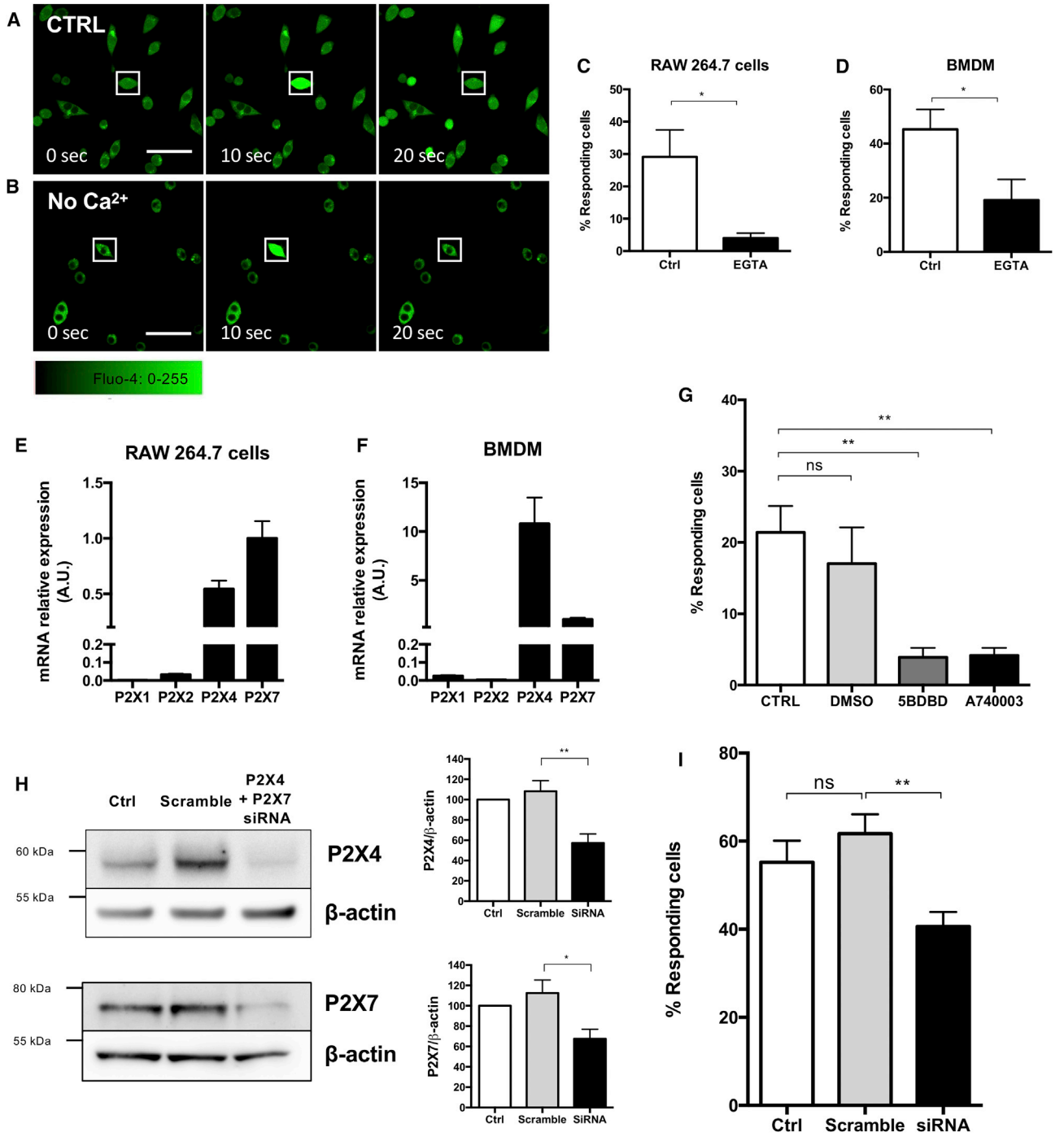

Figure 2. P24XR and P2X7R Mediate ATP-Dependent Calcium Signal Propagation

(A and B) Murine RAW 264.7 macrophages were loaded with photoactivable caged-IP_3 and the fluorescent calcium indicator Fluo-4 (green), and calcium signal propagation after IP_3 uncaging in the origin cell (white box) was monitored in live imaging. Experiments were performed in HBSS with 2 mM Ca^{2+} (A) or in calcium-free HBSS supplemented with 2 mM EGTA (B). Scale bars, 50 μm. See also Video S4.

(C and D) Quantification of 3 independent live calcium imaging experiments with RAW 264.7 (C) or primary BMDMs (D). Error bars represent SEM. For statistical data analysis, Student's t test was used (*$p < 0.05$).

(E and F) Relative mRNA expression of different members of the P2X family of receptors, measured by real-time PCR in the RAW 264.7 cell line (E) and in BMDM primary macrophages (F). Error bars represent SEM.

(legend continued on next page)

effort, we were not able to completely abolish P2X4R and P2X7R expression and obtained a mild reduction only (Figure 2H), with no significant effects on calcium signal propagation (data not shown). However, when the expression of both receptors was reduced, we observed the inhibition of ATP-based paracrine communication, as measured by calcium signal propagation (Figure 2I). Altogether, these results indicate that both P2X4R and P2X7R mediate the paracrine propagation of calcium signals in murine macrophages.

Pro-inflammatory M1 Macrophages Propagate Calcium Signals

In order to gain more insight into the functional significance of ATP paracrine communication, we assessed the expression of purinergic receptors by two different subsets of macrophages: interferon γ (IFNγ)-stimulated "pro-inflammatory" macrophages (M1), and interleukin 4 (IL4)-stimulated "anti-inflammatory" macrophages (M2). Although the total quantity of P2X4R and P2X7R is similar among the different subsets, as assessed by western blot (Figure S3A), we observed an induction of both P2X4R and P2X7R expression at the cell surface in the M1 population (Figure 3A). Thus, we speculated that M1 macrophages may efficiently use ATP for cell-to-cell communication. In agreement, when performing live calcium imaging experiments, we detected a very strong response to ATP-dependent paracrine signaling in IFNγ-treated macrophages (Figures 3B–3D), which is efficiently inhibited by extracellular apyrase (Figure S3B).

Thus, M1 macrophages express at the cell surface high levels of P2X4/P2X7 receptors and are highly efficient in propagating ATP-dependent calcium signals.

Extracellular ATP Is Required for Efficient Phagocytosis

One of the best characterized effector functions exerted by macrophages is the phagocytosis of pathogens, a crucial event for the initiation of the innate and adaptive immune responses. Several studies have suggested a role for calcium during the ingestion of phagocytosed material by macrophages (Demaurex and Guido, 2017; Guido et al., 2015; Hishikawa et al., 1991; Nunes and Demaurex, 2010; Tejle et al., 2002; Wang et al., 2017).

Using microbial molecules conjugated with a pH-sensitive fluorophore (pHrodo) (Figures S4A and S4B), we observed a reduction in the phagocytic capacity of macrophages when extracellular or intracellular calcium is chelated with EGTA or BAPTA, respectively (Figures 4A and 4B).

Thus, we speculated that ATP-dependent paracrine signaling could represent an alert response to potentiate pathogen phagocytosis.

Macrophage phagocytic capacity was markedly reduced in the absence of extracellular ATP, obtained by adding apyrase into the extracellular medium (Figure 4C). The role of extracellular ATP was not specific for a single pathogen, as apyrase inhibited the phagocytosis of molecules of different microbial origin—Gram-negative (*E. coli*) and Gram-positive (*S. aureus*) bacteria and yeast (Zymosan, derived from *S. cerevisiae*) (Figure 4C)—as well as the phagocytosis of apoptotic cells (Figure S4C).

The antagonists of purinergic receptors P2X4 and P2X7 also inhibited macrophage phagocytic capacity, both alone and in combination, indicating that extracellular ATP regulates phagocytosis through the activity of its receptors (Figure 4D). Interestingly, the incubation of macrophages with the ATP-analogous BzATP, a potent P2X7 agonist, did not enhance their phagocytic capacity, suggesting that the endogenous ATP produced by macrophages is sufficient to support the phagocytic process (Figure S4D).

Altogether, these results indicate that, in response to stimuli, macrophages release ATP in the extracellular space that potentiates phagocytosis of target particles by neighboring cells.

Mesenchymal-Stem-Cell-Derived Extracellular Vesicles Express CD39 and Inhibit Phagocytosis

Once in the extracellular space, ATP may be metabolized by the ectonucleotidases CD39 and CD73, which dephosphorylate ATP to AMP and adenosine, thus providing a regulatory mechanism to terminate purinergic signaling (Antonioli et al., 2013). Ectonucleotidases—in particular, CD39—are expressed by different cell types characterized by immuno-suppressive potential, such as mesenchymal stem cells (MSCs) (de Oliveira Bravo et al., 2016). Therefore, we speculated that MSCs, through the expression of the ATP-hydrolyzing enzyme CD39, might regulate macrophage functionality and inhibit phagocytosis.

We and others have shown that the immunosuppressive function of MSCs is largely mediated by secreted factors (Wang et al., 2018; Zanotti et al., 2016), and several studies have recently revealed the prominent role of MSC-derived extracellular vesicles (EVs) (Katsuda et al., 2013). By performing western blot analysis on murine MSC-derived EVs, we detected the expression of CD39 (Figure S4E). Thus, we performed the *in vitro* phagocytosis assay and observed that MSC-derived EVs inhibit macrophage phagocytosis. Importantly, the inhibitory effect of MSC-derived EVs on the phagocytic process was reverted when EVs were pre-incubated with the ectonucleotidase inhibitor ARL-67516 (Figure 4E).

These results highlight how ATP-dependent paracrine communication could be exploited by MSCs to control the phagocytosis process.

DISCUSSION

The importance of ATP as an extracellular signaling molecule was established several decades ago, first in neurons and subsequently in other cell types (Burnstock et al., 2010). An

(G) Quantification of 5 independent live calcium imaging experiments with RAW 264.7 cells pre-treated with the P2X4R inhibitor 5BDBD (100 μM, 30 min at 37°C), the P2X7R inhibitor A740003 (100 μM, 30 min at 37°C), or their vehicle (DMSO) or left untreated. Error bars represent SEM. For statistical data analysis, One-way ANOVA followed by Bonferroni's multiple comparisons test was used (**$p < 0.01$; ns, non-significant).
(H) Representative western blot (left) and quantification of repeated experiments (right) of P2X4R and P2X7R expression in RAW 264.7 cells transfected with siRNA specific for P2X4R and P2X7R or with scramble siRNA. Control cells were electroporated in the absence of oligonucleotides.
(I) Quantification of 3 independent live calcium imaging experiments with RAW 264.7 cells silenced for P2X4R and P2X7R. Error bars represent SEM. For statistical data analysis, one-way ANOVA followed by Bonferroni's multiple comparisons test was used (**$p < 0.01$; ns, non-significant).

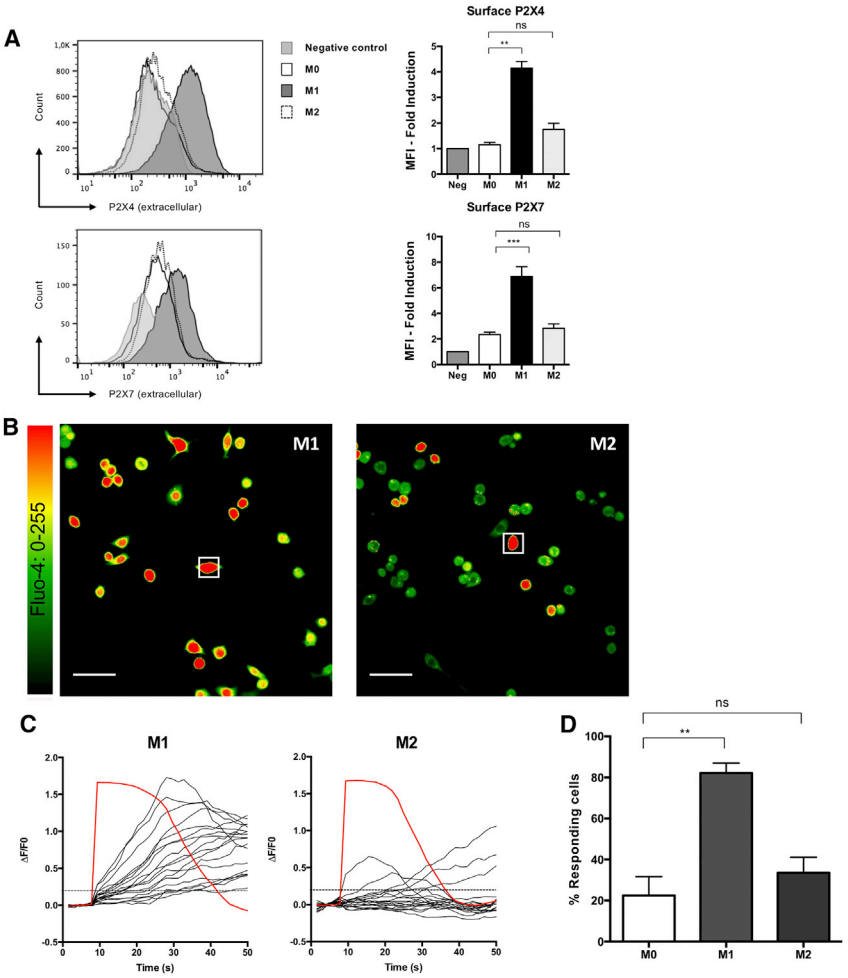

Figure 3. Macrophage Polarization Status Affects Calcium Signal Propagation

(A) The surface expression of P2X4R (top) and P2X7R (bottom) was analyzed by flow cytometry in resting, IFNγ-treated (10 ng/mL, 24 h), or IL4-treated (20 ng/mL, 24 h) macrophages. Histograms show the quantification 3 independent biological replicates. Error bars represent SEM. For data analysis, one-way ANOVA followed by Bonferroni's multiple comparisons test was used (ns, non-significant; $^{**}p < 0.01$; $^{***}p < 0.001$).

(B) Maximal back-projection of two representative live calcium imaging experiments performed with IFNγ- or IL4-treated RAW 264.7 cells loaded with caged-IP_3 and Fluo-4. The fluorescence variation 60 s after the irradiation of the origin cell (white box) is represented in false colors.

(C) Representative traces of live calcium imaging experiments, showing the fluorescence variation after the uncaging of the origin cell (red) and the bystander macrophages (black).

(D) Quantification of 3 independent live calcium imaging experiments. Error bars represent SEM. For data analysis, one-way ANOVA followed by Bonferroni's multiple comparisons test was used ($^{**}p < 0.01$; ns, non-significant).

important role for purinergic signaling has been highlighted in the context of inflammation (Idzko et al., 2014). Indeed, large quantities of ATP are released by injured or necrotic cells and act as a danger-associated molecular pattern (DAMP), recognized by immune cells—in particular, by macrophages—through their purinergic receptors. Macrophages express several purinergic receptors, with P2X7R being the most studied member of the family. Extensive literature shows that ATP-mediated activation of P2X7R is necessary for the maturation and release of IL1β by activated macrophages (Di Virgilio, 2007; Ferrari et al., 1997; Riteau et al., 2012). The process is mediated by the assembly of NLRP3-inflammasome and the activation of caspase-1 and depends on the efflux of intracellular potassium through P2X7R (Pelegrin et al., 2008; Pétrilli et al., 2007). Furthermore, P2X7R activation in macrophages has also been associated with the killing of intracellular bacteria (Coutinho-Silva et al., 2007) and the release of other immunomodulatory factors (Jacob et al., 2013). In addition to the well-described effects of extracellular ATP in the inflammatory microenvironment, several studies also support an autocrine role of ATP (Junger, 2011); in particular, in regulating macrophage chemotaxis (Kronlage et al., 2010) or macrophage activation (Sakaki et al., 2013).

We recently demonstrated that ATP can also be exploited as a paracrine signaling molecule by T lymphocytes (Wang et al., 2014). Intercellular communication is, indeed, crucial for the organization and coordination of immune responses (Rivera et al., 2016). In this work, we investigated the potential role of purinergic signaling in the communication between macrophages and demonstrated that triggered macrophages release ATP and generate calcium signals in untriggered, bystander cells through the activation of P2X4 and P2X7 receptors. P2X4R function in macrophage biology is still poorly defined. A few studies suggest that P2X4R acts as a regulator of P2X7R function or propose the existence of P2X4R-P2X7R heteromers (Kawano et al., 2012; Pérez-Flores et al., 2015; Weinhold et al., 2010). Here, we show that both the receptors are involved in the paracrine spreading of calcium signals. Whether this is due to independent or cooperative signaling is to be defined.

We found that P2X4R and P2X7R are expressed by lymph node subcapsular sinus macrophages and that macrophages propagate ATP-dependent calcium signals within lymph nodes. Interestingly, live calcium imaging experiments highlighted that, after the triggering of a single macrophage in the lymph node slice, an impressive ATP-mediated calcium signaling spreading occurs, involving not only the surrounding macrophages but also other cells, presumably B lymphocytes. Indeed, all immune cells express purinergic receptors and are, therefore, able to respond to extracellular nucleotides (Burnstock, 2016), and B lymphocytes, in particular, have been shown to express several members of the P2X family (Sluyter et al., 2001). It has

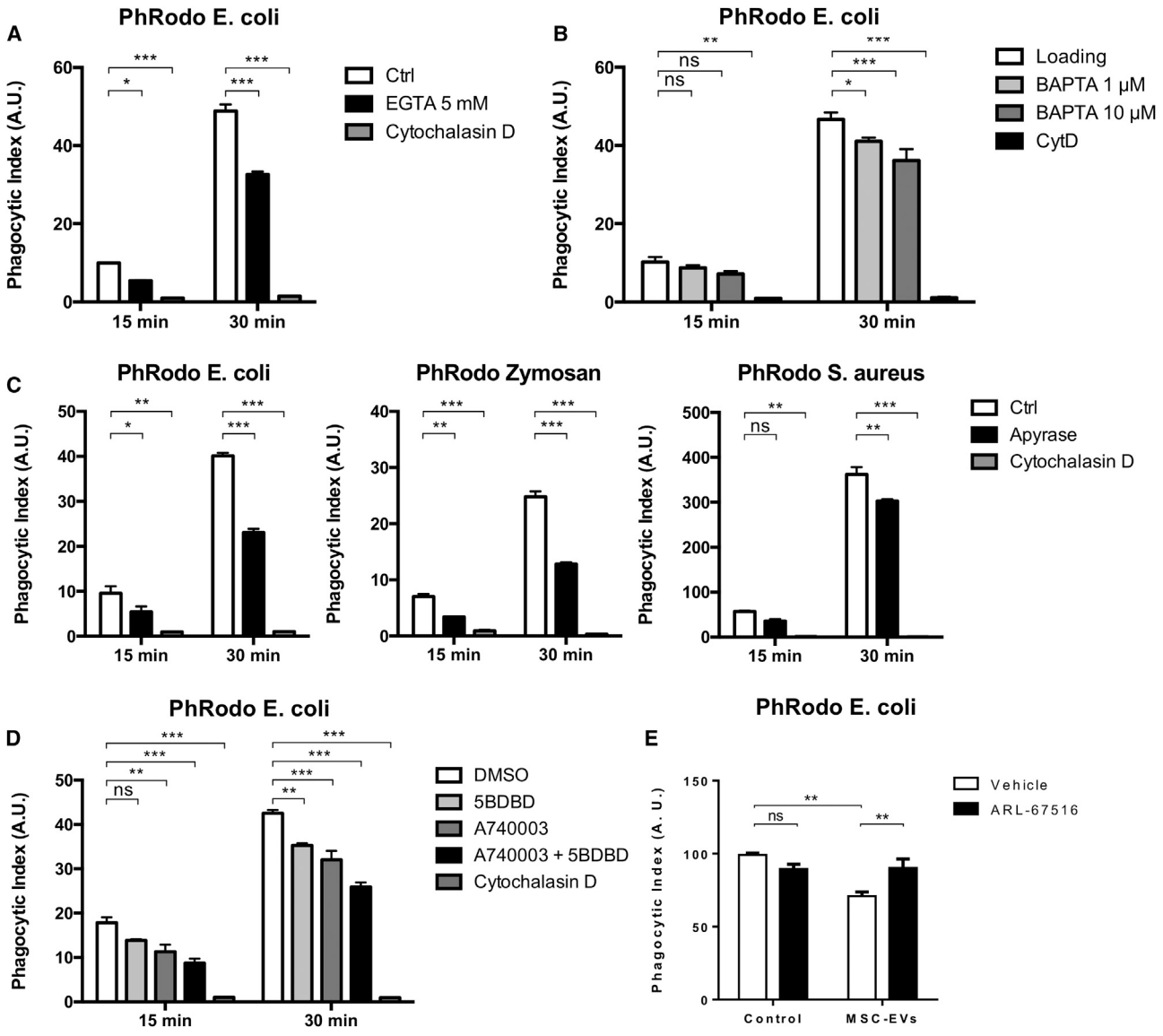

Figure 4. Extracellular ATP Is Required for Efficient Phagocytosis

(A) Primary BMDMs were incubated with PhRodo *E. coli* fluorescent bioparticles in the presence or absence of 5 mM EGTA to chelate extracellular calcium. Phagocytosis was monitored at 15 or 30 min by flow cytometry (see Figure S4). Macrophages incubated with 20 μM cytochalasin D were used as negative reference. The phagocytic index was calculated as the percentage of fluorescent macrophages multiplied by their mean of fluorescence (MFI) and normalized on the cytochalasin-treated samples.

(B) Primary BMDMs were loaded with the intracellular calcium chelator BAPTA-AM or its vehicle (loading solution) before performing the phagocytosis assay.

(C) Primary BMDMs were incubated with PhRodo *E. coli*, PhRodo Zymosan, or PhRodo *S. aureus* fluorescent bioparticles, in the presence or absence of apyrase (5 U/mL).

(D) Primary BMDMs were pretreated with the P2X4R inhibitor 5BDBD (100 μM), the P2X7R inhibitor A740003 (100 μM), or their vehicle (DMSO), or were left untreated, before performing the phagocytosis assay.

(E) Phagocytosis was performed for 30 min in the presence or absence of MSC-derived EVs, pre-incubated or not with ARL-67516 (30 min, 200 μM).

The graphs are representative of at least 3 independent biological replicates, each performed in technical triplicate. Error bars represent SEM. For data analysis, a two-way ANOVA followed by Tukey's multiple comparisons test was used (*$p < 0.05$; **$p < 0.01$; ***$p < 0.001$; ns, non-significant).

been observed that P2X7R activation is linked to the inhibition of BCR signaling (Pippel et al., 2015); however, the role of purinergic signaling in B cells is currently under-investigated. Thus, together with our previous observation on ATP-dependent calcium signals in T cells (Wang et al., 2014), our findings suggest that controlled ATP release may allow the paracrine exchange of information between different immune cell types. Further studies are needed to establish the functional significance of this intercellular communication, for example, in the context of lymph node.

Macrophages are remarkably plastic and can change their functional phenotype depending on the environmental cues they receive. Although recent studies have established that several different macrophage subtypes exist, the classical categorization opposes pro-inflammatory M1 macrophages to anti-inflammatory M2 macrophages (Murray et al., 2014). We observed by flow cytometry that M1 macrophages over-expose P2X4R and P2X7R at the extracellular surface in comparison to M2 or unstimulated (M0) macrophages. Accordingly, we found that M1 macrophages are more efficient in propagating calcium signals, as they respond in higher numbers to the punctual triggering of a single cell. Importantly, M0, M1, and M2 macrophages display comparable levels of total P2X4R and P2X7R proteins, suggesting that IFN-γ stimulation regulates the receptors' localization. Studies in other cells propose that P2X4R and P2X7R membrane localization is regulated by post-translational modifications, by the association with lipid rafts, or through vesicle exocytosis (Gonnord et al., 2009; Hu et al., 2002; Toyomitsu et al., 2012; Weinhold et al., 2010). Our results point toward the functional relevance of P2X4/7R localization; in particular, in the context of macrophage polarization.

Purinergic P2X4 and P2X7 receptors, once activated, mediate a regulated calcium flux inside the cell. Cytosolic calcium oscillations are well known for regulating many cellular functions. In the case of macrophages, several studies indicate that cytosolic calcium is modulated during the phagocytic process (Nunes and Demaurex, 2010).

We observed that the phagocytic rate of *E. coli*-derived fluorescent bioparticles is inhibited when calcium is removed, either intracellularly or extracellularly. Thus, we hypothesized that the release of extracellular ATP by triggered macrophages, resulting in cytosolic calcium elevation in neighboring cells, potentiates phagocytosis. Accordingly, a recent study has shown that ATP supplementation promotes phagocytosis and results in increased bacterial clearance in a mouse model of peritonitis (Ren et al., 2014). Our data show that the phagocytic capacity of macrophages is reduced in presence of the ATP-hydrolyzing enzyme apyrase, as well as of P2X4/7R inhibitors, indicating that extracellular ATP is required for sustaining and boosting an efficient phagocytic process. Importantly, this effect is not specific for a particular pathway of particle recognition, as indicated by the fact that the phagocytosis of bioparticles derived from various microbial sources and the phagocytosis of apoptotic cells were similarly affected by apyrase.

Interestingly, it has been observed that calcium influx generated following the phagocytosis of apoptotic bodies is linked to the generation of an ''innate immune memory,'' which affects macrophage response to subsequent stimuli (Weavers et al., 2016). It would be of interest to investigate the long-term effects of the ATP paracrine signaling in macrophages, also considering how differentially polarized macrophages modulate purinergic receptors' expression.

The importance of the paracrine effect of ATP has also been described in the context of chemotaxis: it has been shown that ATP, together with UTP, is released by apoptotic cells and acts as a chemoattractive molecule for phagocytes via the P2Y2 receptor (Elliott et al., 2009). Moreover, several papers have shown that ATP functions as an autocrine signal that sustains the migration of neutrophils, dendritic cells, and macrophages (Chen et al., 2006; Kronlage et al., 2010; Sáez et al., 2017).

Importantly, calcium fluxes are known to be regulated at the leading edge of migrating phagocytes, ensuring the local regulation of different signaling pathways (Beerman et al., 2015; Evans and Falke, 2007; Ziemba and Falke, 2018). These observations, together with our findings, indicate that purinergic and calcium signaling must be finely regulated to ensure the efficient recruitment of phagocytes to their site of action and the subsequent elimination of invading pathogens and/or apoptotic cells.

The signaling mediated by extracellular ATP is negatively regulated by ectonucleotidases, ATP-degrading enzymes that play a crucial role during inflammation (Antonioli et al., 2013). Ectonucleotidases—in particular, CD39—are expressed by different cell types as MSCs, which are characterized by strong immunosuppressive properties. Moreover, MSC-derived EVs have been the focus of intensive research, due to their outstanding therapeutic potential (Katsuda et al., 2013). Here, we show that EVs derived from murine MSCs express CD39 and decrease macrophage phagocytic potential by degrading extracellular ATP. Altogether, our results identify CD39 enzymatic activity as a relevant player in the control of macrophage phagocytic response and also identify MSCs as potential regulators of this fundamental macrophage effector function.

In conclusion, our data propose an additional role for ATP in innate immunity through the paracrine potentiation of phagocytosis. This mechanism represents a target for the immunosuppressive activity of CD39-expressing cells by degrading extracellular ATP and inhibiting phagocytosis.

STAR★METHODS

Detailed methods are provided in the online version of this paper and include the following:

- KEY RESOURCES TABLE
- CONTACT FOR REAGENT AND RESOURCE SHARING
- EXPERIMENTAL MODEL AND SUBJECT DETAILS
  - Cells
  - Mice
- METHOD DETAILS
  - Confocal calcium imaging
  - *Ex vivo* lymph node preparation and calcium imaging
  - Image analysis
  - RNA and Real-Time PCR
  - Gene Silencing
  - Protein extraction and western blotting
  - Flow cytometry
  - *In vitro* phagocytosis assay of pHrodo bioparticles
  - *In vitro* phagocytosis assay of apoptotic cells
  - Purification of MSC-derived extracellular vesicles (EVs)
- QUANTIFICATION AND STATISTICAL ANALYSIS

SUPPLEMENTAL INFORMATION

Supplemental Information can be found online at https://doi.org/10.1016/j.celrep.2019.03.011.

ACKNOWLEDGMENTS

The authors want to thank the European Union's Seventh Framework Programme for research, technological development, and demonstration under grant agreement no. 602363 to A.V., the ERC Advance Grant under grant agreement no. 322823 to A.V., and the AIRC foundation under grant agreement no. IG 18581 to F.D.V.

AUTHOR CONTRIBUTIONS

A.V. and S.Z. conceptualized the study and wrote the manuscript. S.Z., B.C., and F.M. performed the experiments and analyzed the data. R.A. purified and analyzed extracellular vesicles from mesenchymal stem cells. F.D.V. and B.M. interpreted the results and provided conceptual advice.

DECLARATION OF INTERESTS

The authors declare no competing interests.

Received: August 22, 2018
Revised: December 26, 2018
Accepted: March 1, 2019
Published: April 2, 2019

REFERENCES

Antonioli, L., Pacher, P., Vizi, E.S., and Haskó, G. (2013). CD39 and CD73 in immunity and inflammation. Trends Mol. Med. *19*, 355–367.

Beerman, R.W., Matty, M.A., Au, G.G., Looger, L.L., Choudhury, K.R., Keller, P.J., and Tobin, D.M. (2015). Direct in vivo manipulation and imaging of calcium transients in neutrophils identify a critical role for leading-edge calcium flux. Cell Rep. *13*, 2107–2117.

Beyer, E.C., and Steinberg, T.H. (1991). Evidence that the gap junction protein connexin-43 is the ATP-induced pore of mouse macrophages. J. Biol. Chem. *266*, 7971–7974.

Burnstock, G. (2016). P2X ion channel receptors and inflammation. Purinergic Signal. *12*, 59–67.

Burnstock, G., and Knight, G.E. (2017). Cell culture: complications due to mechanical release of ATP and activation of purinoceptors. Cell Tissue Res. *370*, 1–11.

Burnstock, G., Fredholm, B.B., North, R.A., and Verkhratsky, A. (2010). The birth and postnatal development of purinergic signalling. Acta Physiol. (Oxf.) *199*, 93–147.

Burow, P., Klapperstück, M., and Markwardt, F. (2015). Activation of ATP secretion via volume-regulated anion channels by sphingosine-1-phosphate in RAW macrophages. Pflugers Arch. *467*, 1215–1226.

Carrasco, Y.R., and Batista, F.D. (2007). B cells acquire particulate antigen in a macrophage-rich area at the boundary between the follicle and the subcapsular sinus of the lymph node. Immunity *27*, 160–171.

Chen, Y., Corriden, R., Inoue, Y., Yip, L., Hashiguchi, N., Zinkernagel, A., Nizet, V., Insel, P.A., and Junger, W.G. (2006). ATP release guides neutrophil chemotaxis via P2Y2 and A3 receptors. Science *314*, 1792–1795.

Cohen, H.B., Briggs, K.T., Marino, J.P., Ravid, K., Robson, S.C., and Mosser, D.M. (2013). TLR stimulation initiates a CD39-based autoregulatory mechanism that limits macrophage inflammatory responses. Blood *122*, 1935–1945.

Cotrina, M.L., Lin, J.H., and Nedergaard, M. (1998). Cytoskeletal assembly and ATP release regulate astrocytic calcium signaling. J. Neurosci. *18*, 8794–8804.

Coutinho-Silva, R., Ojcius, D.M., Górecki, D.C., Persechini, P.M., Bisaggio, R.C., Mendes, A.N., Marks, J., Burnstock, G., and Dunn, P.M. (2005). Multiple P2X and P2Y receptor subtypes in mouse J774, spleen and peritoneal macrophages. Biochem. Pharmacol. *69*, 641–655.

Coutinho-Silva, R., Monteiro da Cruz, C., Persechini, P.M., and Ojcius, D.M. (2007). The role of P2 receptors in controlling infections by intracellular pathogens. Purinergic Signal. *3*, 83–90.

de Oliveira Bravo, M., Carvalho, J.L., and Saldanha-Araujo, F. (2016). Adenosine production: a common path for mesenchymal stem-cell and regulatory T-cell-mediated immunosuppression. Purinergic Signal. *12*, 595–609.

Demaurex, N., and Guido, D. (2017). The role of mitochondria in the activation/maintenance of SOCE: membrane contact sites as signaling hubs sustaining store-operated Ca^{2+} entry. In Store-Operated Ca2+ Entry (SOCE) Pathways, K. Groschner, W. Graier, and C. Romanin, eds. (Springer), pp. 277–296.

Di Virgilio, F. (2007). Liaisons dangereuses: P2X(7) and the inflammasome. Trends Pharmacol. Sci. *28*, 465–472.

Elliott, M.R., Chekeni, F.B., Trampont, P.C., Lazarowski, E.R., Kadl, A., Walk, S.F., Park, D., Woodson, R.I., Ostankovich, M., Sharma, P., et al. (2009). Nucleotides released by apoptotic cells act as a find-me signal to promote phagocytic clearance. Nature *461*, 282–286.

Evans, J.H., and Falke, J.J. (2007). Ca2+ influx is an essential component of the positive-feedback loop that maintains leading-edge structure and activity in macrophages. Proc. Natl. Acad. Sci. USA *104*, 16176–16181.

Ferrari, D., Chiozzi, P., Falzoni, S., Dal Susino, M., Melchiorri, L., Baricordi, O.R., and Di Virgilio, F. (1997). Extracellular ATP triggers IL-1 beta release by activating the purinergic P2Z receptor of human macrophages. J. Immunol. *159*, 1451–1458.

Feske, S., Wulff, H., and Skolnik, E.Y. (2015). Ion channels in innate and adaptive immunity. Annu. Rev. Immunol. *33*, 291–353.

Gonnord, P., Delarasse, C., Auger, R., Benihoud, K., Prigent, M., Cuif, M.H., Lamaze, C., and Kanellopoulos, J.M. (2009). Palmitoylation of the P2X7 receptor, an ATP-gated channel, controls its expression and association with lipid rafts. FASEB J. *23*, 795–805.

Guido, D., Demaurex, N., and Nunes, P. (2015). Junctate boosts phagocytosis by recruiting endoplasmic reticulum Ca2+ stores near phagosomes. J. Cell Sci. *128*, 4074–4082.

Guthrie, P.B., Knappenberger, J., Segal, M., Bennett, M.V., Charles, A.C., and Kater, S.B. (1999). ATP released from astrocytes mediates glial calcium waves. J. Neurosci. *19*, 520–528.

Hishikawa, T., Cheung, J.Y., Yelamarty, R.V., and Knutson, D.W. (1991). Calcium transients during Fc receptor-mediated and nonspecific phagocytosis by murine peritoneal macrophages. J. Cell Biol. *115*, 59–66.

Hu, B., Senkler, C., Yang, A., Soto, F., and Liang, B.T. (2002). P2X4 receptor is a glycosylated cardiac receptor mediating a positive inotropic response to ATP. J. Biol. Chem. *277*, 15752–15757.

Idzko, M., Ferrari, D., and Eltzschig, H.K. (2014). Nucleotide signalling during inflammation. Nature *509*, 310–317.

Jacob, F., Pérez Novo, C., Bachert, C., and Van Crombruggen, K. (2013). Purinergic signaling in inflammatory cells: P2 receptor expression, functional effects, and modulation of inflammatory responses. Purinergic Signal. *9*, 285–306.

Junger, W.G. (2011). Immune cell regulation by autocrine purinergic signalling. Nat. Rev. Immunol. *11*, 201–212.

Junt, T., Moseman, E.A., Iannacone, M., Massberg, S., Lang, P.A., Boes, M., Fink, K., Henrickson, S.E., Shayakhmetov, D.M., Di Paolo, N.C., et al. (2007). Subcapsular sinus macrophages in lymph nodes clear lymph-borne viruses and present them to antiviral B cells. Nature *450*, 110–114.

Katsuda, T., Kosaka, N., Takeshita, F., and Ochiya, T. (2013). The therapeutic potential of mesenchymal stem cell-derived extracellular vesicles. Proteomics *13*, 1637–1653.

Kawano, A., Tsukimoto, M., Noguchi, T., Hotta, N., Harada, H., Takenouchi, T., Kitani, H., and Kojima, S. (2012). Involvement of P2X4 receptor in P2X7 receptor-dependent cell death of mouse macrophages. Biochem. Biophys. Res. Commun. *419*, 374–380.

Khakh, B.S., and Burnstock, G. (2009). The double life of ATP. Sci. Am. *301*, 84–90, 92.

Kronlage, M., Song, J., Sorokin, L., Isfort, K., Schwerdtle, T., Leipziger, J., Robaye, B., Conley, P.B., Kim, H.-C., Sargin, S., et al. (2010). Autocrine purinergic receptor signaling is essential for macrophage chemotaxis. Sci. Signal. *3*, ra55.

Li, W., Llopis, J., Whitney, M., Zlokarnik, G., and Tsien, R.Y. (1998). Cell-permeant caged InsP3 ester shows that Ca2+ spike frequency can optimize gene expression. Nature *392*, 936–941.

Lim, J.J., Grinstein, S., and Roth, Z. (2017). Diversity and versatility of phagocytosis: roles in innate immunity, tissue remodeling, and homeostasis. Front. Cell. Infect. Microbiol. *7*, 191.

Murray, P.J., Allen, J.E., Biswas, S.K., Fisher, E.A., Gilroy, D.W., Goerdt, S., Gordon, S., Hamilton, J.A., Ivashkiv, L.B., Lawrence, T., et al. (2014). Macrophage activation and polarization: nomenclature and experimental guidelines. Immunity *41*, 14–20.

Nunes, P., and Demaurex, N. (2010). The role of calcium signaling in phagocytosis. J. Leukoc. Biol. *88*, 57–68.

Osipchuk, Y., and Cahalan, M. (1992). Cell-to-cell spread of calcium signals mediated by ATP receptors in mast cells. Nature *359*, 241–244.

Pelegrin, P., Barroso-Gutierrez, C., and Surprenant, A. (2008). P2X7 receptor differentially couples to distinct release pathways for IL-1beta in mouse macrophage. J. Immunol. *180*, 7147–7157.

Pellegatti, P., Falzoni, S., Pinton, P., Rizzuto, R., and Di Virgilio, F. (2005). A novel recombinant plasma membrane-targeted luciferase reveals a new pathway for ATP secretion. Mol. Biol. Cell *16*, 3659–3665.

Pérez-Flores, G., Lévesque, S.A., Pacheco, J., Vaca, L., Lacroix, S., Pérez-Cornejo, P., and Arreola, J. (2015). The P2X7/P2X4 interaction shapes the purinergic response in murine macrophages. Biochem. Biophys. Res. Commun. *467*, 484–490.

Pétrilli, V., Papin, S., Dostert, C., Mayor, A., Martinon, F., and Tschopp, J. (2007). Activation of the NALP3 inflammasome is triggered by low intracellular potassium concentration. Cell Death Differ. *14*, 1583–1589.

Pippel, A., Beßler, B., Klapperstück, M., and Markwardt, F. (2015). Inhibition of antigen receptor-dependent Ca(2+) signals and NF-AT activation by P2X7 receptors in human B lymphocytes. Cell Calcium *57*, 275–289.

Ren, H., Teng, Y., Tan, B., Zhang, X., Jiang, W., Liu, M., Jiang, W., Du, B., and Qian, M. (2014). Toll-like receptor-triggered calcium mobilization protects mice against bacterial infection through extracellular ATP release. Infect. Immun. *82*, 5076–5085.

Riteau, N., Baron, L., Villeret, B., Guillou, N., Savigny, F., Ryffel, B., Rassendren, F., Le Bert, M., Gombault, A., and Couillin, I. (2012). ATP release and purinergic signaling: a common pathway for particle-mediated inflammasome activation. Cell Death Dis. *3*, e403.

Rivera, A., Siracusa, M.C., Yap, G.S., and Gause, W.C. (2016). Innate cell communication kick-starts pathogen-specific immunity. Nat. Immunol. *17*, 356–363.

Sáez, P.J., Vargas, P., Shoji, K.F., Harcha, P.A., Lennon-Duménil, A.-M., and Sáez, J.C. (2017). ATP promotes the fast migration of dendritic cells through the activity of pannexin 1 channels and $P2X_7$ receptors. Sci. Signal. *10*, eaah7107.

Sakaki, H., Tsukimoto, M., Harada, H., Moriyama, Y., and Kojima, S. (2013). Autocrine regulation of macrophage activation via exocytosis of ATP and activation of P2Y11 receptor. PLoS ONE *8*, e59778.

Schneider, C.A., Rasband, W.S., and Eliceiri, K.W. (2012). NIH Image to ImageJ: 25 years of image analysis. Nat. Methods *9*, 671–675.

Sim, J.A., Park, C.-K., Oh, S.B., Evans, R.J., and North, R.A. (2007). P2X1 and P2X4 receptor currents in mouse macrophages. Br. J. Pharmacol. *152*, 1283–1290.

Sluyter, R., Barden, J.A., and Wiley, J.S. (2001). Detection of P2X purinergic receptors on human B lymphocytes. Cell Tissue Res. *304*, 231–236.

Tejle, K., Magnusson, K.-E., and Rasmusson, B. (2002). Phagocytosis and phagosome maturation are regulated by calcium in J774 macrophages interacting with unopsonized prey. Biosci. Rep. *22*, 529–540.

Toyomitsu, E., Tsuda, M., Yamashita, T., Tozaki-Saitoh, H., Tanaka, Y., and Inoue, K. (2012). CCL2 promotes P2X4 receptor trafficking to the cell surface of microglia. Purinergic Signal. *8*, 301–310.

Underhill, D.M., Gordon, S., Imhof, B.A., Núñez, G., and Bousso, P. (2016). Élie Metchnikoff (1845–1916): celebrating 100 years of cellular immunology and beyond. Nat. Rev. Immunol. *16*, 651–656.

Wang, C.M., Ploia, C., Anselmi, F., Sarukhan, A., and Viola, A. (2014). Adenosine triphosphate acts as a paracrine signaling molecule to reduce the motility of T cells. EMBO J. *33*, 1354–1364.

Wang, Y., Subramanian, M., Yurdagul, A., Jr., Barbosa-Lorenzi, V.C., Cai, B., de Juan-Sanz, J., Ryan, T.A., Nomura, M., Maxfield, F.R., and Tabas, I. (2017). Mitochondrial fission promotes the continued clearance of apoptotic cells by macrophages. Cell *171*, 331–345.e22.

Wang, M., Yuan, Q., and Xie, L. (2018). Mesenchymal stem cell-based immunomodulation: properties and clinical application. Stem Cells Int. *2018*, 3057624.

Weavers, H., Evans, I.R., Martin, P., and Wood, W. (2016). Corpse engulfment generates a molecular memory that primes the macrophage inflammatory response. Cell *165*, 1658–1671.

Weinhold, K., Krause-Buchholz, U., Rödel, G., Kasper, M., and Barth, K. (2010). Interaction and interrelation of P2X7 and P2X4 receptor complexes in mouse lung epithelial cells. Cell. Mol. Life Sci. *67*, 2631–2642.

Xiang, Y., Wang, X., Yan, C., Gao, Q., Li, S.-A., Liu, J., Zhou, K., Guo, X., Lee, W., and Zhang, Y. (2013). Adenosine-5′-triphosphate (ATP) protects mice against bacterial infection by activation of the NLRP3 inflammasome. PLoS ONE *8*, e63759.

Yang, D., He, Y., Muñoz-Planillo, R., Liu, Q., and Núñez, G. (2015). Caspase-11 requires the pannexin-1 channel and the purinergic P2X7 pore to mediate pyroptosis and endotoxic shock. Immunity *43*, 923–932.

Zanotti, L., Sarukhan, A., Dander, E., Castor, M., Cibella, J., Soldani, C., Trovato, A.E., Ploia, C., Luca, G., Calvitti, M., et al. (2013). Encapsulated mesenchymal stem cells for in vivo immunomodulation. Leukemia *27*, 500–503.

Zanotti, L., Angioni, R., Calì, B., Soldani, C., Ploia, C., Moalli, F., Gargesha, M., D'Amico, G., Elliman, S., Tedeschi, G., et al. (2016). Mouse mesenchymal stem cells inhibit high endothelial cell activation and lymphocyte homing to lymph nodes by releasing TIMP-1. Leukemia *30*, 1143–1154.

Ziemba, B.P., and Falke, J.J. (2018). A PKC-MARCKS-PI3K regulatory module links Ca2+ and PIP3 signals at the leading edge of polarized macrophages. PLoS ONE *13*, e0196678.

Zsembery, A., Boyce, A.T., Liang, L., Peti-Peterdi, J., Bell, P.D., and Schwiebert, E.M. (2003). Sustained calcium entry through P2X nucleotide receptor channels in human airway epithelial cells. J. Biol. Chem. *278*, 13398–13408.

STAR★METHODS

KEY RESOURCES TABLE

REAGENT or RESOURCE	SOURCE	IDENTIFIER
Antibodies		
Rat anti-mouse anti-CD169-AlexaFluor647 (clone 3D6.112)	Biorad	Cat# MCA884; RRID: AB_322416
Rabbit anti-mouse anti-P2X4R (extracellular)	Alomone labs	Cat# Apr-024; RRID: AB_2341050
Rabbit anti-mouse anti-P2X7R (extracellular)	Alomone labs	Cat# Apr-008; RRID: AB_2040065
Rat anti-mouse anti-CD39 (clone Duha-59)	Biolegend	Cat# 143801; RRID: AB_11203887
Rat anti-mouse anti-CD63 (clone R5G2)	MBL International	Cat# D263-3; RRID: AB_1278815
Biological Samples		
Mesenchymal Stem Cell-derived Extracellular Vesicles	This lab	N/A
Chemicals, Peptides, and Recombinant Proteins		
iso-Ins(1,4,5)P_3/PM (caged)	Enzo Life Sciences	Cat# ALX-307-071-C100
Fluo-4-AM	ThermoFisher Scientific	Cat# F14201
Apyrase from potatoes	Sigma Aldrich	Cat# A6535
A-740003	Tocris	Cat# 3701
5-BDBD	Tocris	Cat# 3579
2′(3′)-O-(4-Benzoylbenzoyl)adenosine 5′triphosphate triethylammonium salt (Bz-ATP)	Sigma Aldrich	Cat# B6396
BAPTA, AM, cell permeant chelator	ThermoFisher Scientific	Cat# B6769
Critical Commercial Assays		
pHrodo Green *E. coli* BioParticles Conjugate for Phagocytosis	ThermoFisher Scientific	Cat# P35366
pHrodo Green Zymosan Bioparticles Conjugate for Phagocytosis	ThermoFisher Scientific	Cat# P35365
pHrodo Green S. aureus Bioparticles Conjugate for Phagocytosis	ThermoFisher Scientific	Cat# P35367
Cell Line V Nucleofector Amaxa kit	Lonza	Cat# VACA-1003
Experimental Models: Cell Lines		
Raw 264.7	ATCC	Cat# TIB-71
B16F10	ATCC	Cat# CRL-6475
Experimental Models: Organisms/Strains		
C57BL/6J mice	Internal breeding	N/A
Oligonucleotides		
Silencer Select Pre-designed siRNAs for P2X4R	Ambion	Cat# S71184; s71185
Silencer Select Pre-designed siRNAs for P2X7R	Ambion	Cat# S71187; s71189
Silencer Select Negative Control No. 1 siRNA	Ambion	Cat# 4390843
Primers for real-time PCR (see table in Methods)	This paper	N/A
Software and Algorithms		
ImageJ (for image analysis)	Schneider et al., 2012	N/A
FlowJo	FlowJo, LLC	https://www.flowjo.com/
Other		
Amicon® Ultra 15 mL Filters	Merck Millipore	Cat# UFC910096

CONTACT FOR REAGENT AND RESOURCE SHARING

Further information and requests for resources and reagents should be directed to and will be fulfilled by the Lead Contact, Sara Zumerle (sara.zumerle@unipd.it).

EXPERIMENTAL MODEL AND SUBJECT DETAILS

Cells

The murine RAW 264.7 cell line was cultured in DMEM 4,5 g/L glucose supplemented with 2 mM L-glutamine, 1 mM sodium pyruvate, 100 U/ml penicillin, 100 U/ml streptomycin (Lonza), and 10% Fetal Bovine Serum (FBS, GIBCO).

The murine melanoma B16F10 cell line was cultured in RPMI supplemented with 2mM L-glutamine, 1 mM sodium pyruvate, 100 U/ml penicillin, 100 U/ml streptomycin (Lonza) 0.1% β-mercaptoethanol and 10% Fetal Bovine Serum (FBS, GIBCO).

Bone marrow-derived macrophages (BMDMs) were obtained from bone marrow precursor cells. Briefly, femurs and tibiae were collected from 8-12 week old C57BL/6J mice. Bone marrow was flushed with IMDM supplemented with 100 U/ml penicillin, 100 U/ml streptomycin (Lonza), and 10% FBS Superior (Millipore) and red blood cells were removed using ACK lysis buffer (Lonza). 50000 cells/cm^2 were seeded on low-adhesion plates in complete medium supplemented with 40 ng/ml murine M-CSF (Miltenyi Biotech). M-CSF was replenished after 4 days in culture. Experiments were performed at day 7-8. In some experiments, at day 6-7 the cell culture medium was replaced with fresh medium containing 10 ng/ml mIFNγ (Miltenyi) or 20 ng/ml mIL-4 (Miltenyi) to induce the polarization into M1 or M2 status, respectively.

Murine Mesenchymal Stem Cells (MSCs) were isolated as previously described (Zanotti et al., 2013). Briefly, femurs and tibiae were collected from 8 week-old, C57BL/6 female mice; the bone marrow was flushed and cultured in 25 cm^2 tissue culture flasks at a concentration of 2x10^6 cells/cm^2 using complete Dulbecco modified Eagle medium low glucose (DMEM, Lonza) supplemented with 20% heat-inactivated fetal bovine serum (Biosera), 2 mM glutamine (Lonza), 100 U/ml penicillin/streptomycin (Lonza). After 48 hours, the non-adherent cells were removed. After reaching 70%–80% confluence, the adherent cells were harvested and expanded in larger flasks.

Mice

C57BL/6J mice were kept in regular light and dark cycles, with unrestricted access to water and food. Mice were kept under Italian national and EU directives (2010/63/EU) for animal research with protocols approved by institute Ethical Committee and the Italian Ministry of Health (1045/2016-PR approved on 26/10/2016).

METHOD DETAILS

Confocal calcium imaging

Murine macrophages previously plated on glass coverslips were loaded with the cell membrane permeable ester of caged-IP_3-PM (1 μM, Enzo Life Science) and the calcium indicator Fluo-4-AM (5 μM, Molecular Probes), Pluronic F-127 (0.1%, w/v, Life Technologies), sulphinpyrazone (250 μM) in unsupplemented culture medium for 30 minutes at 37°C. Live calcium imaging was performed in imaging buffer (Hank's Balanced Salt Solution supplemented with Ca^{2+} 2 mM, Lonza) using a Zeiss LSM700 laser scanning confocal microscope. Time-lapse images were acquired for 1 minute (0.6 frame/sec), using a 40X water immersion objective (Zeiss W Plan-Apochromat 40x/1.0 DIC M27). Fluo-4-AM was excited with a 488-nm laser (0.5% power). Regions of interest (ROIs) were drawn on one distinct cell per field; the UV laser (405 nm, 100% power, 10 ms pulse) was used to release active IP_3 within the ROI. Images were analyzed using ImageJ software (Schneider et al., 2012). Fluo-4 traces were generated by averaging pixel signals within the ROIs, and normalized on the baseline fluorescence of the first 5 frames ($\Delta F/F_0$). Control experiments were performed using murine macrophages loaded with calcium indicator alone.

In some experiments, the imaging solution was supplemented with 5 U/ml apyrase (Sigma Aldrich), 100 μM A740003 (Sigma Aldrich), 100 μM 5BDBD (Tocris), 100 μM BzATP (Sigma Aldrich) or in Ca^{2+}-free HBSS supplemented with 2 mM EGTA (Sigma Aldrich).

Ex vivo lymph node preparation and calcium imaging

C57BL/6J mice were injected with 1 μg of Alexa647-conjugated anti-CD169 antibody (Biorad) in the footpad. After 45 minutes, mice were sacrificed and popliteal lymph nodes were collected and embedded in 4% low-melt agarose (Sigma Aldrich).

200 μm slices were cut with a vibratome in a saline solution containing 150 mM NaCl, 10 mM HEPES–NaOH, 5 mM D–glucose, 5 mM KCl, 2 mM $CaCl_2$, 2 mM sodium pyruvate, 1 mM $MgCl_2$ (pH 7.2, 310 mOsm). The slices were loaded with caged-IP_3-PM (1 μM, Enzo Life Science), Fluo-4-AM (5 μM, Molecular Probes), Pluronic F-127 (0.1%, w/v, Life Technologies), sulphinpyrazone (250 μM) in unsupplemented phenol red-free IMDM (GIBCO) for 30 minutes at 37°C. Live calcium imaging was performed in phenol red-free IMDM using a Zeiss LSM700 laser scanning confocal microscope. Time-lapse images were acquired for at least 1 minute (0.6 frame/sec), using a 40X water immersion objective (Zeiss W Plan-Apochromat 40x/1.0 DIC M27). Fluo-4-AM was excited with a 488-nm laser (0.5% power). Regions of interest (ROIs) were drawn on one distinct CD169-positive macrophage per field; the UV laser (405 nm, 100% power, 20 ms pulse) was used to release active IP_3 within the ROI. Apyrase (5 U/ml, Sigma) was added to the imaging buffer in some of the experiments. We have observed calcium waves in C57BL/6J murine LNs despite the known DNA polymorphism in the *p2x7* gene that reduces receptor function. LN slides loaded with Fluo-4-AM only (without caged-IP_3) were negative controls for calcium wave.

Image analysis

For the analysis of calcium signaling events, one ROI per cell was designed and single cell Fluo-4 traces were generated by averaging pixel signals within the ROIs, and normalized on the baseline fluorescence of the first 5 frames ($\Delta F/F_0$) using ImageJ software. A cell was considered as "Responding cell" when its fluorescence variation increased more than 20% over the baseline ($\Delta F/F_0 \geq 0.2$) in the first 40 s after the uncaging of one single cell. The % of responding cells was calculated as the number of cells showing a $\Delta F/F_0$ value ≥ 0.2 over the total number of cells in each field.

Calcium signaling in viable lymph node slices was analyzed using the same approach; ROIs were designed only on $CD169^+$ cells.

RNA and Real-Time PCR

Total RNA was extracted from macrophages using TriZol reagent (Thermo Fisher Scientific), and cDNA synthetized from 200 ng of RNA using the High Capacity RT kit (Applied Biosystems), according to the manufacturers' instructions. Real-Time PCR was performed using Sybr Green I (Applied Biosystems) on a 7900HT Fast Real-Time PCR System (Applied Biosystems), with the primers indicated in the table. Gene expression was normalized on RPLP0 expression.

Name	Forward primer 5′-3′	Reverse primer 5′-3′
Rplp0	GGGCATCACCACGAAAATCTC	CTGCCGTTGTCAAACACCT
P2X1R	ATCTTTGGCTGGTGTCCTGTAG	TGACCTTGAAGCGTGGAAAG
P2X2R	AGGACGCTGTGTACCCTATTAC	TTTCAGAAGTCCCATCCTCCAC
P2X4R	GCAGAAAACTTCACCCTCTTGG	AGGTAGGAGGTGGTAATGTTGG
P2X7R	GCAGGGGAACTCATTCTTTGTC	TCCACCCCTTTTTACAACGC

Gene Silencing

P2X4 and P2X7 gene expression was transiently knocked down transfecting RAW 264.7 cells with Silencer Select Pre-designed siRNAs (Ambion) specific for P2X4 (s71184; s71185) and/or P2X7 (s71187; s71189). Silencer Select Negative Control No. 1 siRNA (Ambion) was adopted as scramble. Transfection was performed with Cell Line V Nucleofector Amaxa kit (Lonza), according to the manufacturer's instructions. All siRNAs were used at the final concentration of 50 nM. The silencing efficiency was controlled by western blot.

Protein extraction and western blotting

Total protein lysates from macrophages were obtained using RIPA buffer (1mM EDTA, 150 mM NaCl, 1% NP-40, 0.1% SDS, 0.5% Sodium deoxycholate, 50 mM Tris HCl, Protease inhibitors cocktail, pH 8). The protein concentration was quantified with the BCA assay (Euroclone), according to the manufacturer's instructions. 30 μg of total lysates were resuspended in NuPAGE LDS Loading Buffer (Thermo Fisher Scientific) supplemented with 50 mM DTT and boiled at 99°C for 5 minutes. Samples were loaded in NuPAGE 4%–12% Bis-Tris Gels (Thermo Fisher Scientific) and Western Blot analysis was performed using standard methods. Anti-P2X4R (Alomone Labs), anti-P2X7R (Alomone Labs) and anti-β-actin (Abcam) primary antibodies were used. Immunoblots were acquired with the ImageQuantLS camera and analyzed with ImageJ Software.

Flow cytometry

Macrophages were detached using PBS supplemented with 2mM EDTA and resuspended in the staining solution (PBS supplemented with 2% FBS). For lymph node cell analysis, single cell suspensions were obtained from murine lymph nodes by passing cells through 40-μm cell strainers.

After counting, cells were incubated with anti-CD16/CD32 (BD PharMingen), and subsequently stained with the appropriate combinations of the following antibodies: anti-Cd11b-PerCP Cy5.5 (M1/70, BD Biosciences), anti-CD169-AlexaFluor647 (MOMA-1, Biorad), anti-P2X7R-extracellular-FITC (Alomone Labs), purified anti-P2X4R-extracellular (Alomone Labs) followed by incubation with the secondary anti-rabbit-FITC antibody (Thermo Fisher). When indicated, appropriate isotype control antibodies were used to discriminate for antibody specificity. Stained cells were analyzed with a FACSCanto II instrument (BD Biosciences). FlowJo software was used for data analysis.

In vitro phagocytosis assay of pHrodo bioparticles

In vitro phagocytosis was assessed with Alexa Fluor 488-Zymosan, *E. coli* or S. aureus PhRodo bioparticles (Molecular Probes). Bone marrow-derived macrophages were starved in suspension in IMDM supplemented with 0.2% Bovine Serum Albumin (Sigma Aldrich), for 40 minutes at 37°C. After 15 minutes on ice, cells were incubated with bioparticle suspension (100 ng bioparticles/100000 cells) at 37°C. Cells pretreated for 30 minutes with 20 μM Cytochalasin D (Calbiochem) were used as negative control. For some experiments, 5 U/ml apyrase, 100 μM A740003, 100 μM 5BDBD, 5 mM EGTA, 200 μM ARL-67516 were added during the experiment. For intracellular calcium chelation, macrophages were loaded with 10 μM BAPTA-AM (Thermo Fisher Scientific) in starvation medium at 37°C for 30 minutes.

Phagocytosis was stopped after 15 or 30 minutes by placing cells on ice. The fluorescence of non-internalized beads was quenched using Trypan blue and the samples were analyzed by flow cytometry with a FACSCanto II flow cytometer (BD Bioscience). The phagocytic index was scored as percentage of Alexa Fluor 488-positive macrophages multiplied by their mean of fluorescence (MFI) and normalized on the Cytochalasin-treated samples.

In vitro phagocytosis assay of apoptotic cells

For induction of apoptosis, murine B16F10 cells were detached using 0.25% Trypsin-2mM EDTA and loaded with 5 μM Calcein green (ThermoFisher) for 30 min at 37°C in serum free medium. Cells were then washed and heated at 56°C for 10 min. After heat-shock, 2 mM staurosporine was added and cells were kept in incubator for at least 1 hour. Before apoptotic cells (AC) phagocytosis, apoptosis was assessed using APC-Annexin V (eBioscience). Apoptosis was generally over the 95%.

Bone marrow-derived macrophages were starved in suspension in IMDM supplemented with 0.2% Bovine Serum Albumin (Sigma Aldrich), for 40 minutes at 37°C. During starvation, macrophages were loaded with 5 μM DDAO-1 (ThemoFisher). After 15 minutes on ice, cells were incubated with apoptotic cells at the ratio of 10 apoptotic cells to 1 macrophage at 37°C. Apyrase was added at the concentrations of 5 or 10 U/ml. Cells pretreated for 30 minutes with 20 μM Cytochalasin D were used as negative control. After 30 and 60 min, phagocytosis was stopped by diluting cells and cells were then placed on ice until the analysis by flow cytometry. Phagocytosis was assessed by measuring the percentage of Calcein green/DDAO-1 double positive cells. Data were normalized with Cytochalasin D-treated cells.

Purification of MSC-derived extracellular vesicles (EVs)

MSC growth medium was substituted with DMEM low glucose supplemented with 10% FBS, 2mM glutamine, 100 U/ml penicillin/streptomycin for 24 hours. Subsequently, the medium was changed with DMEM low glucose supplemented with 2 mM glutamine, 100 U/ml penicillin/streptomycin for the 18 hours. Conditioned medium was harvested and centrifuged at 4000 rpm for 10 min.

Extracellular Vesicles (EVs) were isolated from MSC-conditioned medium by ultrafiltration using Amicon® Ultra 15 mL Filters (Merck Millipore) following manufacturer's instructions. Briefly, each tube was first sterilized with 70% ethanol and then washed two times by centrifuging it at 4000 g for 10 minutes. Subsequently, 12 mL of MSC-conditioned medium were loaded into the tube and centrifuged at 2800 g per 20 minutes at room temperature. After washing the filter with PBS, EVs were collected, concentrated in about 150 μL of PBS, and directly stored at −80°C.

For protein characterization, an additional wash with PBS with 0.4% SDS of the filter membrane was added. Total protein of EVs was quantified by MicroBCA kit (Pierce). From 3 to 5 μg of proteins were separated by 10% SDS-PAGE under non-reductive conditions. Anti-CD63 (MBL), and anti-CD39 (Biolegend) primary antibodies were used.

QUANTIFICATION AND STATISTICAL ANALYSIS

Data analysis was performed using Prism 6 (GraphPad, USA). Sample size was not predetermined by statistical methods. The data distribution was verified by performing Shapiro-Wilk normality test. Student's t test was used to compare two groups and one-way ANOVA followed by Bonferroni post hoc test was used to compare three or more groups, as indicated in figure legends. Statistical significance was taken at $p < 0.05$ and indicated with asterisks in the figures (ns = non-significant; * = $p < 0.05$; ** = $p < 0.01$; *** = $p < 0.001$). The n number for each experiment has been stated in figure legends, and represents the number of independent biological replicates. When using samples derived from animals, n represents the number of animals.